Journal of Drug Delivery Science and Technology 51 (2019) 552–558

Contents lists available at ScienceDirect

Journal of Drug Delivery Science and Technology

journal homepage: www.elsevier.com/locate/jddst

Pyridine Ruthenium(III) complexes entrapped in liposomes with enhanced cytotoxic properties in PC-3 prostate cancer cells

Angela D'Amora[a,b,c], Maria Elena Cucciolito[b,c], Roberta Iannitti[d], Giancarlo Morelli[a], Rosanna Palumbo[d], Francesco Ruffo[b,c], Diego Tesauro[a,*]

[a] Dipartimento di Farmacia and CIRPeB Università degli studi di Napoli Federico II & Diagnostica e Farmaceutica Molecolari S.C.R.L (DFM), Via Mezzocannone,16, I-80134, Napoli, Italy
[b] Dipartimento di Scienze Chimiche, Università degli studi di Napoli Federico II, Complesso Universitario di Monte S. Angelo, Via Cintia 21, I-80126, Napoli, Italy
[c] Consorzio Interuniversitario di Reattività Chimica e Catalisi, via Celso Ulpiani 27, 70126, Bari, Italy
[d] Istituto di Biostrutture e Bioimmagini – CNR, Via Mezzocannone 16, I-80134, Naples, Italy

ARTICLE INFO

Keywords:
Egg l-α-phosphatidylcholine cholesterol
DSPE-PEG liposome
Inorganic complexes delivery
Pyridine ruthenium (III) complexes
PC-3 prostate cancer cells

ABSTRACT

The first aim of the present study is the development of a new ruthenium(III) complex, belonging to NAMI-A class, with a potentially high cytotoxic ability. The presence of a fully protected sugar moiety as ruthenium ligand should increase the complex ability to cross cellular membranes. Furthermore, it sets this molecule in the area of biocompatible agents as tumor drug. The second, more relevant, purpose is to verify the ruthenium complexes activity after loading into liposomes. We reported the characterization and in vitro biological assays of pyridine derivatives of ruthenium complexes loaded into Egg L-α-phosphatidylcholine cholesterol/DSPE-PEG liposomes. Dynamic light scattering estimates that the sizes of all obtained liposomes are in the 100 nm range. This value is suitable for in vivo use. The loading ability and release kinetic allowed selecting the best ratio between the lipid fraction and metal to be tested in cellular experiments. The growth inhibitory effects of both liposomal and free complex in PC-3 prostate cancer cell lines demonstrate a high cytotoxic ability of the liposome entrapped ruthenium (III) complex suggesting additional role further the antimetastatic function.

1. Introduction

Metal-based anticancer drugs fulfill an important role in the fight against cancer pathologies. The first metal complex approved for clinical use by FDA was Cisplatin (CDDP) in 1978 [1]. Since then, platinum based drugs are pivotal drugs for treatment of many human tumours like testicular and ovarian cancers and nowadays Cisplatin is one of the three top-selling chemotherapeutic drugs. However, the chemiotherapic use of platinum complexes is strongly limited by many and severe side effects and acquired tumor resistance [2–5]. These limits pushed researchers and pharma companies to develop other complexes of transition metals [6,7]. Among them, a prominent role is occupied by ruthenium complexes in the oxidation states II and III [8–11]. In principle, these compounds offer several advantages: first of all some Ru (III)-based derivatives act against cancer cells that were resistant to platinum compounds following a different mechanism of action [12]. The research was focused on two complexes: imidazolium [trans-$RuCl_4$(1H-imidazole)(DMSO-S)] (NAMI-A) [13,14] and indazolium [trans-$RuCl_4$(1H-indazole)$_2$] (KP1019) [15]. NAMI-A was validated against lung metastases of a number of solid metastasizing tumours, including a NSCLC of human origin engrafted in the nude mouse [16–19], but it does not show cytotoxic activity in the 60-cell-line NCI panel for in vitro anticancer drug screening [20]. On the other hand KP1019 acts as cytotoxic drug, effective against primary tumours as colorectal tumours [21], and recently it has been shown that it also likely act as an antimetastatic agent [22]. Both complexes overcame the early stage in clinical trials [13,15].

The promising properties of ruthenium complexes can be attributed to ligands exchange in biological media. NMR studies carried out in the last decades provided evidence that the coordination of Ru is deeply transformed in physiological conditions: NAMI-A undergoes both chloride and DMSO hydrolysis while forming a mixture of hydrolyzed species in about 15 min [23]. This is the first step in protein binding of all ruthenium complexes. Indeed, in most of experiments carried out (e.g. serum albumin adducts formation [24]) it was observed the loss of original ligands coordinated to the metal center [25,26].

All results seem to agree that NAMI-A acts like a pro-drug, even if the integrity of ruthenium complexes is essential to store the cytotoxic

* Corresponding author.
E-mail address: dtesauro@unina.it (D. Tesauro).

https://doi.org/10.1016/j.jddst.2019.02.009
Received 27 September 2018; Received in revised form 12 February 2019; Accepted 12 February 2019
Available online 27 March 2019
1773-2247/ © 2019 Elsevier B.V. All rights reserved.

activity because its metabolites interact mainly with cell membrane and are not significantly internalized by cells [27,28]. In contrast, the presence in both cytosol and in the nuclear region of ruthenium centers generated by KP1019 was demonstrated by X-ray fluorescence imaging. This occurrence increases cytotoxic activity, compared to NAMI-A [29]. The detected outcome is due to slower extracellular degradation allowing enhanced cellular uptake through passive diffusion.

In this scenario the condition of administration of ruthenium drugs seems crucial to exploit their anticancer activity. Indeed, in the last years innovative strategies have been developed to vehicle ruthenium ions in tumor cells. They could be summarized in three main opportunities. First, ruthenium centers can be coordinated by bioactive ligands or by ligands bearing a bioactive molecule able to drive the entire complex toward tumor cells [30,31]; the second opportunity is that ruthenium complexes are endowed with a chemical moiety able to polymerize or to promote formation of supramolecular aggregates [32–34]; and the last possibility is that in which ruthenium complexes can be physical encapsulated in nanoparticles [35]. In the first two strategies the cytotoxic activity of ruthenium drugs enhances compared with NAMI-A but in both cases deep modifications are required on ligand structures. Although introduction of new moieties did not affect in most of the case the electronic properties and the rate of ligand exchanges in physiological conditions, increasing the drug efficacy, the protocol to begin a clinical evaluation requires more heavy procedures. The third strategy allows to preserve the same drug structure and to increase stability in aqueous solutions. Moreover, like the second approach, the nanoparticle formulation facilitated cellular accumulation. Therefore loading in nanoparticles was pursued for Cisplatin by increasing the cytotoxic effects and reducing resistance phenomena [36]. Currently, a liposomal formulation based on 1,2-dipalmitoylphosphatidylglycerol (DPPG) (Lipoplatin™ traded by Regulon Inc, MountainView, CA) [37] reaches the latter phase in clinical trials. Despite these positive results to the best of our knowledge only KP1019 was entrapped in Poly(lactic acid) nanoparticles with Pluronic F68 and Tween 80 surfactants. This formulation shows enhanced cytotoxic activity [33].

Our study aims to incorporate ruthenium complexes in the inner aqueous compartment of liposomes and to test biological properties of two NAMI-A like pyridine derivatives. Recently Walsby's group synthesized NAMI-A analogues modifying the axial pyridine ligand that is pivotal for the features of the ruthenium complexes, demonstrating that the growth of lipophilicity enhances in vitro cytotoxicity [38–40]. Inspired by these evidences specifically, in this work we have explored two pyridine derivatives of the sodium-compensated analogue of NAMI-A, Na[*trans*-$RuCl_4$(pyridine)(DMSO)] (RuPy) and Na[*trans*-$RuCl_4$(PyTry)(DMSO)] (RuPyTry) (Fig. 1). In the latter complex the pyridine ligand is functionalized with a fully protected sugar moiety to increase biocompatibility and the ability to cross the cell membrane due the lipophilic moiety. Additionally, carbohydrates allow to provide multiple points of interaction as H-bond donor or acceptor, tuning the hydrophilic properties [41,42].

The liposome was formulated mixing Phosphatidylcholine (PC)/Cholesterol (Chol)/DSPEPeg2000 in molar ratio 57/38/5. This composition was selected reproducing similar composition of other systems already tested in clinical phases such as delivery systems [43].

Moreover, we have assessed the best concentration and the ability to load both complexes. Lastly the cytotoxic properties were tested on PC-3 tumor cells.

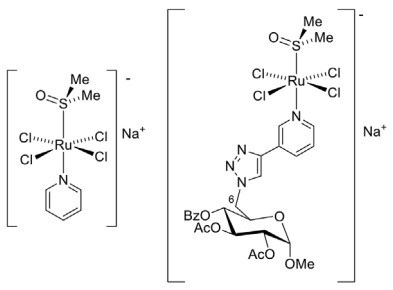

Fig. 1. Chemical structure of the ruthenium complexes RuPy (left) and RuPyTry (right).

2. Materials and methods

Phosphatidylcholine and cholesterol (Chol) were purchased from Avanti Polar Lipids (Alabaster, AL). All the other chemicals were commercially provided by Sigma-Aldrich (Bucks, Switzerland) or LabScan (Stillorgan, Dublin, Ireland) and were used as received unless further purification. $[(DMSO)_2H][trans\text{-}Ru(DMSO)_2Cl_4]$ [44], Na^+ $[trans\text{-}Ru(DMSO)_2Cl_4]$ [44], $Na[Ru(Py)(DMSO)Cl_4]$ (RuPy) [34] and PyTry [45] were synthesized as previously described. All the aqueous solutions were prepared by weight adding MilliQwater. The products were characterized by ^{1}HNMR spectroscopy. The spectra were recorded with a Bruker AVANCE 400 spectrometer. FTIR spectra were acquired by Jasco FT/IR 4100 (Easton, MD, USA). Liposomes were extruded using a thermo barrel extruder system (Northern Lipids Inc, Vancouver, BC, Canada). Inductively Coupled Plasma atomic emission Mass Spectroscopy (ICP-MS) (ICP SPECTRO Arcos with End On Plasma torch; Spectro Analytical, Kleve, Germany) equipped with a capillary cross-flow nebulizer.

2.1. Synthetic procedures

2.1.1. Synthesis of Na[Ru(PyTry)(DMSO)Cl_4] - (RuPyTry) complex

PyTry ligand (65 mg, 0.118 mmol) was added to a suspension of freshly prepared [Na][*trans*-$RuCl_4(DMSO)_2$] (50 mg, 0.118 mmol) in acetone (4 mL). The mixture was stirred at 40 °C and the reaction was monitored by TLC on alumina. After 4 h the solvent was removed under reduced pressure, giving the desired salt in pure form (yield > 95%).

IR: 2915 cm^{-1}, 2850 (DMSO) 1748 (C=O) 1632 (C=C) 1414 1235 MS: (CH_3OH) 830 *m/z*. (M^{+1}) MS (H_2O) 819 *m/z* (M-$2Cl^-$ + $2H_2O$ + Na^+), 797 *m/z* (M-$2Cl^-$ + $2H_2O$ + H^+).

2.1.2. Ruthenium complexes stability

RuPy and RuPyTry complexes were separately dissolved in glass vials in 1.0 mL phosphate buffer solution at pH 7.3 giving molar concentrations of $2.5 \cdot 10^{-3}$ M. The solutions were monitored by UV–Vis spectroscopy for 72 h after their preparation. The stability of these complexes was also evaluated in similarly prepared aqueous solution.

2.2. Liposomes preparation and ruthenium complexes loading

Empty aggregates composed of PC/Chol/DSPEPeg2000 in molar ratio 57/38/5 were formulated by the thin film hydration method. The three molecules were dissolved in MeOH/$CHCl_3$(50/50 v/v) solution and mixed in appropriate amounts. A thin film was obtained by evaporating the organic solvents by slowly rotating the vial containing the solution under a stream of nitrogen. Lipid films were then hydrated in saline solution containing 0.9% w/w of NaCl, sonicated for 30 min and extruded 10 times at room temperature through a polycarbonate membrane with 100 nm pore size, using a thermo-barrel extruder system under N_2. The RuPy and RuPyTry loaded liposome were prepared following the same procedure adding to organic mixture the ruthenium compound dissolved in methanol. Unencapsulated ruthenium complexes were removed by loading the supernatant on pre-equilibrated Sephadex G50 column. Liposomal fractions were collected and analyzed. The drug loading coefficient (DL%, defined as the weight percentage between the loaded ruthenium complexes and the amphiphilic liposome components), the encapsulation ratio (ER%, defined as the weight percentage of ruthenium complex encapsulated in the liposome on the total complex previously added) and the metal contents

were quantified by means of ICP-MS.

2.3. Ruthenium complexes release

1 mL of liposomes loaded with Ru complexes, were formulated at 5 mM concentration as described above and introduced into a dialysis bag (MW cut-off = 3500 Da). The bag was placed into 20 mL of fetal bovine serum and incubated under stirring for 72 h at 37 °C. 2.5 mL of the dialyzed serum solution were replaced with an equivalent amount of fresh serum at different time points. The extent of ruthenium complex release was evaluated by ICP-MS analysis as percentage of the ratio between the amount of released metal and of the total metal previously loaded into the liposomes.

2.4. Dynamic light scattering characterization

Dynamic light scattering (DLS) measurements were carried out using a Zetasizer Nano ZS (Malvern Instruments, Westborough, MA) that employs a 173° backscatter detector.

Other instrumental settings are measurement position (mm): 4.65; attenuator: 8; temperature 25 °C; cell: disposable sizing cuvette. Before starting with DLS measurements, previously prepared samples were diluted at final concentration of $2.0 \cdot 10^{-4}$ M and centrifuged at room temperature at 13.000 rpm for 5 min. For each formulation, RH and P.I. were calculated as the mean of three measurements on three different batches.

2.5. Cell culture and viability assay

Human prostate cancer PC-3 cells were grown in RPMI 1640 medium (GIBCO, USA) supplemented with 10% fetal bovine serum (GIBCO, USA), 1% L-glutammine (LONZA, Belgium). The normal human dermal fibroblasts (NHDF) were purchased from Lonza, seeded on T-25 primary flasks (Beckton Dickinson) and maintained in fibroblast basal medium supplemented with 2% FBS, 1 mg/mL hydrocortisone, 10 ng/mL human epidermal grow factor, 3 ng/mL rh fibroblast growth factor b. Cells were cultured in a humidified 5% carbon dioxide atmosphere at 37 °C and harvested at approximately 90% confluence. Reduction of cell viability was determined by crystal violet assay. Briefly, PC-3 cells (4×10^4/mL) were seeded in 96-well flat-bottom microplates and incubated overnight to allow cell adhesion. Subsequently, culture medium was removed and cells were treated with different concentrations of RuPy and RuPyTry encapsulated in liposomes, and free compounds, in quadruplicate. The absorbance intensity of cell treated with empty liposomes were used as negative control. After 48 h culture medium was removed, cells were washed with Phosphate-Buffered Saline (PBS), fixed and stained with 0,1% (w/v) crystal violet in 25% methanol (Sigma-Aldrich) for 30 min at dark. Then crystal violet was removed and cells were washed twice and let dry. Finally, dye was solubilized by adding 10% (v/v) acetic acid and the amount of dye taken up was quantified with a plate reader (ThermoMultiscan FC) at 595 nm. All data were expressed as mean ± SD.

3. Results and discussion

3.1. Ru complex synthesis

The 1,4-disubstituted-1,2,3-triazole (PyTry) containing a carbohydrate moiety was synthetized exploiting the well-assessed pathway based on click chemistry methods [45]. The synthesis of the Ru(III) complex was carried out adapting the procedure reported for the synthesis of RuPy complex [34].

The ligand PyTry was coordinated to Ru(III) by displacing a DMSO molecule from the Na[trans-Ru(DMSO)$_2$Cl$_4$], affording RuPyTry complex (Fig. 2). This ligand was preferred as compared to 2-ethynylpyridine derivative in order to avoid that the ligand can chelate the ruthenium ion affording to another class of compounds. The complex was isolated in almost quantitative yield and characterized through ESI-MS, IR and ^{1}HNMR spectroscopy.

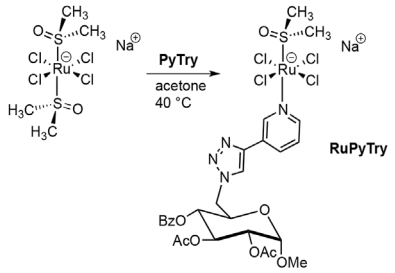

Fig. 2. Synthesis scheme of the sugar bearing ligand complex (RuPyTry).

The RuPyTry complex formation was confirmed by ESI-MS in methanol, while the mass spectrum in water display many signals with the same isotopic pathway. All peaks are attributable to ruthenium complexes obtained by chloride ligands replacement by water molecules (see below).

The paramagnetic ruthenium(III) ion broadens the ^{1}HNMR signals of coordinated ligands, not allowing a standard assignment procedure (The spectrum is reported in supplementary materials). However, the presence of two very broad signals at −1.80 and −12.5 ppm are diagnostic. The first signal is attributed to coordinated pyridine ring and the second is recognized for the methyl of the S-coordinated DMSO. These attributions were assigned by comparison with related Ru (III) − DMSO complexes in literature [10].

3.2. UV–Vis spectroscopic characterization

The hydrolysis of NAMI like Ru(III) complexes occurs by exchanging chloride and DMSO ligands with water molecules. The formation of the aqua complexes is considered essential as these species effectively interact with the in vivo targets [46]. The UV–Vis spectra allow to monitor the reaction following the evolution over time of the chromophores. The spectra were carried out in water and in saline phosphate buffer at different pH and at 2.5 mM concentration. The stability of RuPy has been previously studied [47], while the spectra were carried out again to compare its stability toward the hydrolysis of RuPyTry at the same concentration (Fig. 3). The band centered at 395 nm is attributed to the ligands to Ru charge transfer transition (Ru → Cl CT). For both complexes in saline buffer it gradually reduced in intensity over time, more rapidly for RuPyTry disappearing for the latter complex in ca. 1.30 h *vs* 5 h for RuPy. The simultaneous appearance of a new band centered at 350 nm for both compounds was observed. It reached the highest value at same time which that vanished the 395 nm band. This first step of hydrolysis is attributed to chloride ion substitution with a water molecule [46]. The easy formation of the monoaqua complex of RuPyTry could be favored by the intramolecular hydrogen-bonding properties of nitrogen atom in the triazole moiety of PyTry ligand with the coordinated water molecule. Both mono-aqua compounds evolved in complexes coordinated by a major number of water molecules. This transformation involve the disappearance of the 350 nm centered band.

In aqueous acid solution, at pH < 6, both starting complexes are more stable but if the spectrum of RuPy after 72 h is unaltered, RuPyTry shows a more propensity to undergo hydrolysis.

3.3. Aggregates formulation and DLS characterization

Both anionic ruthenium complexes are clearly soluble in water despite the lipophilic feature of the fully protected glucose moiety. Therefore, the aqueous inner compartment of liposomes could host

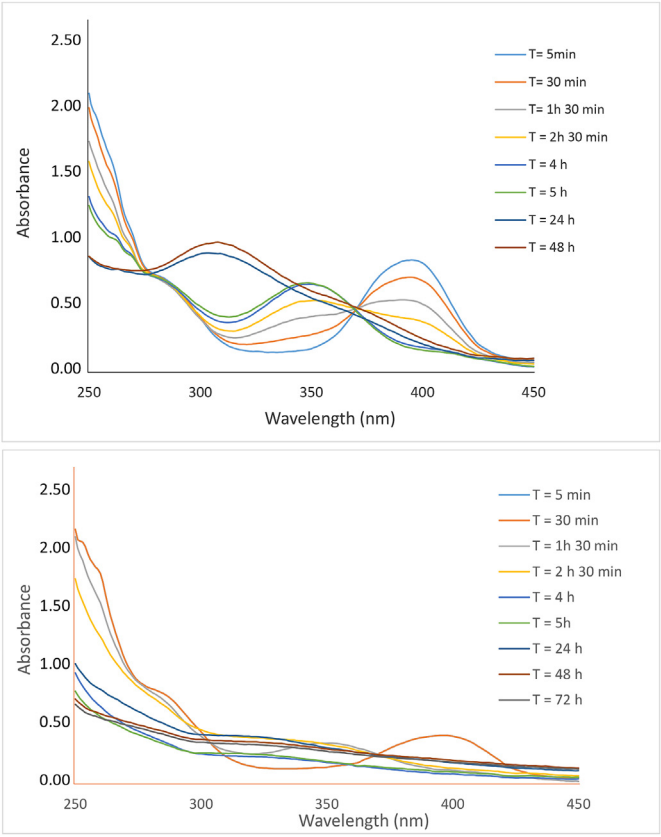

Fig. 3. UV–Vis absorption spectra of RuPy (top) and RuPyTry (bottom), both at 2.5 mM concentration in the saline phosphate buffer (pH 7.3), recorded at different times after dissolution in order to study the complexes stability vs ligands exchange. The RuPyTry complex shows a more rapid evolution. In aqueous acid solution at pH < 6both complexes, as expected, are more stable (spectra not reported).

RuPy and RuPyTry complexes. The surfactants used in liposome formulation are selected to determine their structural properties (size, charge, polydispersity index, in vivo stability, transition temperature) and to influence the drug loading and release properties. On the basis of these consideration the chosen phospholipid was PC (Egg L-a-phosphatidylcholine) which represents a good compromise between saturated or unsaturated phospholipids. The unsaturated bonds increase fluidity and permeability with respect to HSPC used in other preparations and currently tested in clinical phase delivering metal complexes.

Moreover 38% of cholesterol, in order to increase membrane rigidity, and 5% of DSPE-Peg (1,2-distearoyl-sn-glycero-3-phosphoethanolamine) were added to the lipid composition. The presence of flexible PEG chains exposed on the liposome surface prevents liposome interaction with MPS macrophages, increasing the circulation time. All formulations were prepared starting from a lipid film, hydrating it with 0.9% w/w of NaCl by extensive bath sonication. The colloid solutions were extruded at room temperature through a polycarbonate membrane with 100 nm pore size to reduce liposome size. Unilamellar vesicles were obtained. Loading of ruthenium complexes was achieved into liposomes using the passive equilibration loading method. The unloaded complex was removed eluting the supernatant on pre-equilibrated SephadexG50 column. The drug loading contents (DL), measured with respect to the PC phospholipid content, and the encapsulation efficiencies, are reported in Tables 1 and 2. Encapsulation complexes amount was assessed by ICP-MS on the liposomal fraction.

Empty and loaded liposomes were characterized by DLS technique. All data are listed in Table 1. Measurements were performed at a concentration of $5{\cdot}10^{-4}$ molkg^{-1} in water solution. All aggregates show a mono modal distribution indicating the presence of a single population of aggregates. At infinite dilution, R_H value can be reasonably evaluated using the translational diffusion coefficients in the Stokes–Einstein equation [48]. The values are comparable to PC liposomes previously reported when the 100 nm filters are used in the extrusion process [49].

Variations of radius were observed for different lipidic concentrations or containing percentages of ruthenium complexes. The liposomes dimension grows increasing the lipidic concentrations whereas the amount of drug does not significantly affect the diameter of the aggregates. Sizes of all obtained liposomes are suitable for in vivo use. Indeed according to the EPR effect, liposomes of size below 200 nm, extravasate from the blood vessels into the tumor tissue driving the payload [50]. Lipidic concentrations increase the polydispersity. This trend appears to concern above all RuPyTry loaded liposomes (lipoRuPyTry) probably due to the higher DL% compared to lipoRuPy. Nevertheless these values, a PDI of about 0.3, are considered to be acceptable in drug delivery applications using lipid-based carriers [51].

Empty liposomes have an average value of a zeta potential of −12.0 mV with observing slight difference varying the molar phospholipidic concentrations. These values are expected due to liposome composition (57% mol of PC zwitterionic phospholipid and 5 mol % of DSPE-PEG2000 anionic phospholipid). Ruthenium compound loaded liposomes showed the similar values. The presence of the complexes in inner compartment does not significantly alter the zeta potential.

3.4. Drug loading and release

Three different phospholipid concentrations (2, 5 and 10 mM) were investigated. Moreover, different ratios between the above reported phospholipid concentration and the amount of the ruthenium complexes were chosen (0.125, 0.250, 0.500 and 1.00 mmol for 2 mM, 0.500 and 1.00 mmol for 5.0 and 10.0 mM). In Tables 1 and 2 are reported DL% and ER %.

The loaded amount of RuPy complex is lower than that of RuPyTry complex in all conditions. This outcome could be attribute to the presence of the fully protected sugar ligand. The hydrophobic feature of this moiety probably allows stronger interactions within hydrophobic region of the bilayers because of the van der Waals forces. The drug loading coefficient is more broadly influenced for both complexes by two different effects, obviously by the initial amount of complexes and the used lipid concentration, both of them providing an increase of the DL percentage. In particular, for each lipid concentration, a progressive increase of the drug encapsulated was observed for both complexes in 2 mM lipid concentration going from 0.09 to 1.80 for RuPy and from 0.27 to 3.50 for RuPyTry. Moreover, decrease on the DL% was observed by increasing the amount of lipid concentration from 2 mM to 10 mM, respectively, thus maintaining a fix ratio between the lipid concentration and the drug amount.

Hence, we can conclude that an increase of the lipid concentration strength produces a more evident effect on the loading properties of the liposomes.

The release profile of RuPy and RuPyTry from liposomes of both complexes was followed within 72 h, using a dialysis membrane immersed in fetal bovine serum at 37 °C.

We assumed that the crossing of ruthenium complexes through the dialysis membrane happened very fast and that the overall release from liposomes to the dialysis bag medium is the rate determining step. The amount of ruthenium complexes released was estimated by ICP-MS analysis. It is worth noting that very low percentages of complexes are released in serum release (4%) and the main part of them released within 30 h, for both complexes (Fig. 4). The slow release suggests a high affinity of the two ruthenium complexes toward the inner core of liposome.

Table 1
Structural parameters (hydrodynamic radius, PDI and zeta potential from dynamic light scattering measurements) for the different RuPy loaded aggregates. The encapsulation ratios (ER%) and the drug loading coefficients (DL%) are also reported.

sample	Lipid Concentration (mmol/L)	RuPy (mmol) Added	R_H (nm) ± S.D.	PDI	Zeta potential (mV)	DL%	ER%
Lipo e	2	–	45.0 ± 10.6	0.114	−15.3 ± 4.92	–	–
Lipo 1	2	$0.125\ 10^{-3}$	55.0 ± 21.53	0.116	−14.3 ± 4.81	0.09	2.5
Lipo 2	2	$0.250\ 10^{-3}$	62.2 ± 21.31	0.122	−12.3 ± 5.60	0.28	4.0
Lipo 3	2	$0.500\ 10^{-3}$	60.4 ± 25.5	0.135	−13.4 ± 5.20	0.73	5.0
Lipo 4	2	$1.00\ 10^{-3}$	80.2 ± 35.3	0.189	−11.3 ± 4.78	1.80	6.2
Lipo e	5	–	75.0 ± 10.6	0.316	−10.9 ± 4.51	–	–
Lipo 5	5	$0.500\ 10^{-3}$	79.2 ± 38	0.190	−10.9 ± 5.13	0.35	6.0
Lipo 6	5	$1.00\ 10^{-3}$	80.4 ± 40	0.208	−11.7 ± 4.35	0.78	6.8
Lipo e	10	–	98.2 ± 45	0.283	–11.1 ± 4.49	–	–
Lipo 7	10	$0.500\ 10^{-3}$	84.3 ± 42	0.228	−11.9 ± 5.50	0.18	6.2
Lipo 8	10	$1.00\ 10^{-3}$	63.3 ± 26	0.142	−12.9 ± 4.97	0.42	7.2

3.5. Biological assays

The cytotoxicity of Ru compounds were measured on PC-3 cells and the results are summarized in Fig. 5. Ru complexes as free drug 100 μM did not show cytotoxic effect. At further concentration of RuPy and RuPyTry at 500 μM we found 30% and 15% reduction of cell viability respectively. These results are comparable with literature data for RuPy on different cell model [34]. The liposomal formulation assessed after 48 h of treatments showed a significant cytotoxic effects. The highest concentrations of lipoRuPy 3.2 μM and lipoRuPyTry 10 μM reduced the viability of prostatic cells about at 80% and 60% respectively. In contrast free Ru used at a concentration about ten times higher than liposomal formulation were little cytotoxic. In addition, for comparison, treatment with 8.0 μM of cisplatin induced a 50% reduction of cell viability similar to lipoRuPyTry. Whereas lipoRuPy is more active at lower concentrations, (data not reported in figure).

In addition, the effect on cell viability of lipoRuPyTry was assessed on NHDF cells to compare the results obtained on cancer cells.

As showed in Fig. 6 no effect on cell viability was observed in the normal cells. The differences between malignant cells versus normal cells usually were found in studies of ruthenium complexes cytotoxicity [52,53].

Literature data did not report the cytotoxic effect of NAMI-A like complexes on normal cells. Many different causes can explain this behavior, but the reported assays at moment do not allow advancing hypothesis.

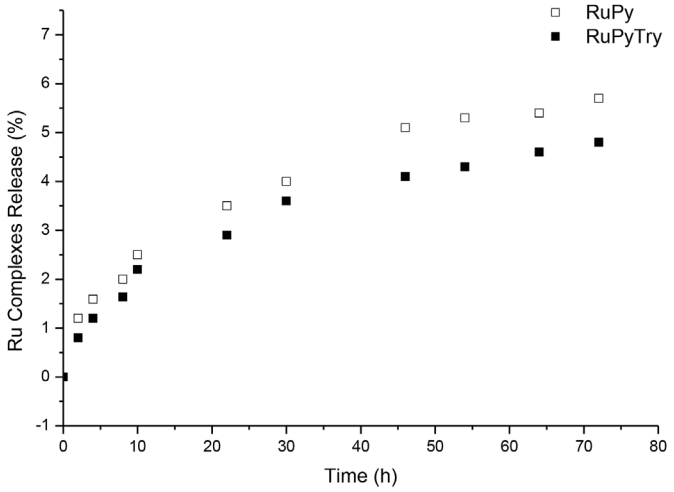

Fig. 4. Release of RuPy and RuPyTry complexes. The amount of Ru complexes released (%) was estimated by ICP.

4. Conclusions

The aim of this paper was to study chemical and biological behavior of two NAMI-A class ruthenium complexes were studied. A new sugar-incorporated Ru(III) complex was designed to increase biocompatibility and the ability to cross the cell membrane. The complex was fully characterized by ^{1}H NMR and UV–Vis spectroscopy to identify the new compound and to compare its ligand exchange properties in water to RuPy. Therefore, both complexes were biologically investigated against PC-3 prostate cancer cells. The cytotoxic properties of RuPyTry were not enhanced when compared to RuPy. The presence of the fully sugar protecting group should increase the ability to cross the cell membrane due the lipophilicity of this moiety but the very fast exchange of chlorido ligand with the water save the hydrophilic behavior of the complex. According to literature data, this property induces a very low cytotoxicity. In order to check if the delivery system inside the cell can modify the biological effect, both complexes were encapsulated in liposomes based on Egg PC and containing cholesterol and DPSE-PEG. The latter components were added to PC to increase the rigidity of the liposome wall and the blood circulation time. Structural data, loading studies and stability measurements allow ensuring stability of these systems. Liposomes fit within a critical radii size range (60–80 nm), the drug loading are comparable with classic formulations of metal drugs. The biological results allow verifying a relevant cytotoxic ability of

Table 2
Structural parameters (hydrodynamic radius, PDI and zeta potential from dynamic light scattering measurements) for the different RuPyTry loaded aggregates. The encapsulation ratios (ER%) and the drug loading coefficients (DL%) are also reported.

SAMPLE	Lipid concentration (mmol/L)	RuPyTry (mmol) Added	R_H (nm) ± S.D.	Zeta potential (mV)	PDI	DL%.	ER%
Lipo A	2	$0.125\ 10^{-3}$	75.7 ± 47.5	−12.5 ± 4.95	0.238	0.27	7.6
Lipo B	2	$0.250\ 10^{-3}$	53.3 ± 18.67	−11.8 ± 5.05	0.089	0.70	10.0
Lipo C	2	$0.500\ 10^{-3}$	76.9 ± 27.26	−12.3 ± 5.08	0.149	1.51	10.7
Lipo D	2	$1.00\ 10^{-3}$	74.2 ± 20.16	−11.5 ± 4.65	0.052	3.54	13.0
Lipo E	5	$0.500\ 10^{-3}$	76.5 ± 40.21	−11.9 ± 4.91	0.352	0.70	12.4
Lipo F	5	$1.00\ 10^{-3}$	84.5 ± 42.19	−11.9 ± 5.40	0.182	2.10	19.0
Lipo G	10	$0.500\ 10^{-3}$	80.3 ± 40.82	−11.2 ± 4.83	0.345	0.42	15.0
Lipo H	10	$1.00\ 10^{-3}$	84.3 ± 40.64	−12.2 ± 5.23	0.311	1.64	29.3

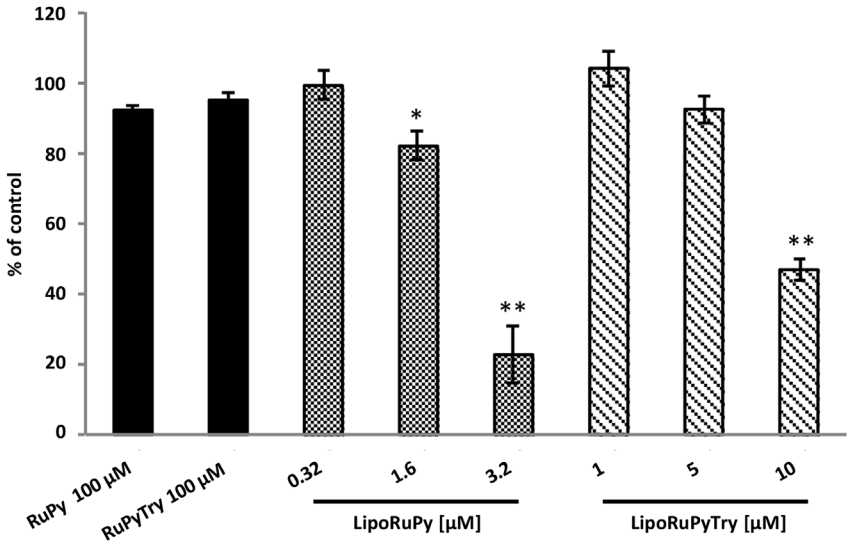

Fig. 5. Dose-response histograms of the cytotoxic effect of ruthenium pyridine complexes in PC-3 cell line. The cell viability was assessed after 48 h treatment with increased doses of complexes. Data are normalized to the value obtained with the untreated cells and are expressed as means of quadruplicate samples ± SD of two independent experiments. *P < 0.05 and **P < 0.002 vs untreated cells.

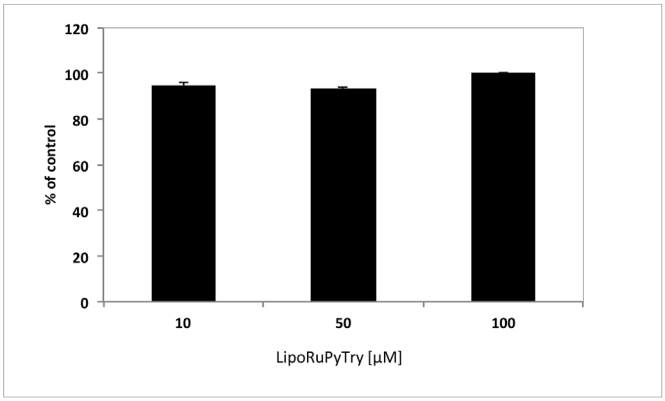

Fig. 6. Determination of the cytotoxic effect of RuPyTry on NHDF. Cells (2×10^4/mL) were treated with different doses of lipoRuPyTry for 48 h. The cell viability, measured by crystal violet assay, is reported as percentage of empty liposomes cell treated. Data represent the means of triplicate samples ± SD of two independent experiments.

both Ru (III) complexes joining to the well demonstrated anti metastatic properties. At the best of our knowledge this is the first case in which a ruthenium (III) complex shows cytotoxic ability higher than cisplatin. Moreover, the lipoRuPyTry preparation is selective toward the malignant cells.

The biological results could be explained making two hypothesis. (1) The loading in the liposome allows that metal center acts inside the cell overcoming the crossing membrane problem. (2) It can be suppose that in the inner liposome compartment, the relative amount of water makes slowest the ligand kinetic exchange. This occurrence preserves longer the ruthenium pro-drug. Unfortunately, the low concentration of the complexes does not allow following the ligand exchange by UV–Vis spectroscopy. We can probably state that both effects could be co-operative and induce the observed behavior.

Conflicts of interest

There are no conflicts to declare.

Acknowledgements

We would like to acknowledge Clementina Mallitti for their assistance in formulation aggregates and in their chemical physical experimental procedures. The Italian "Consorzio Interuniversitario di Ricerca in Chimica dei Metalli nei Sistemi Biologici (CIRCMSB)" is gratefully acknowledged. A.D. thanks Diagnostica e Farmaceutica Molecolari S.C.R.L (DFM) for the grant. This work was supported by MIUR (PRIN2015 - Prot. 20154X9ATP).and by Regione Campani (POR Campania Fers 2014-2020 Project No B61G18000470007) for financial support.

Appendix A. Supplementary data

Supplementary data to this article can be found online at https://doi.org/10.1016/j.jddst.2019.02.009.

References

[1] L. Kelland, The resurgence of platinum-based cancer chemotherapy, Nat. Rev. Canc. 7 (2007) 573–584.
[2] M.E. Howe-Grant, S.J. Lippard, Aqueous platinum(II) chemistry; binding to biological molecules, in: H. Sigel (Ed.), Metal Ions in Biological Systems, vol. XI, M. Dekker, New York, 1980, pp. 63–125.
[3] K.N.J. Burger, R.W.H.M. Staffhorst, B. de Kruijff, Interaction of the anticancer drug cisplatin with phosphatidylserine in intact and semiintact cells, Biochim. Biophys. Acta 1419 (1999) 43–54.
[4] J. Reedijk, Why does cisplatin reach guanine-N7 with competing s-donor ligands available in the cell? Chem. Rev. 99 (1999) 2499–2510.
[5] R. Oun, Y. Moussa, N.J. Wheate, The side effects of platinum-based chemotherapy drugs: a review for chemists, Dalton Trans. 47 (2018) 6645–6653.
[6] M.J. Clarke, F. Zhu, D.R. Frasca, Non-platinum chemotherapeutic metallopharmaceuticals, Chem. Rev. 99 (1999) 2511–2533.
[7] S. Komeda, A. Casini, Next-generation anticancer metallodrugs, Curr. Top. Med. Chem. 12 (2012) 219–235.
[8] R.R.E. Morris, R.E. Aird, P. del Socorro Murdoch, H. Chen, J. Cummings, N.D. Hughes, S. Parsons, A. Parkin, G. Boyd, D.I. Jodrell, P.J. Sadler, Inhibition of cancer cell growth by ruthenium (II) arene complexes, J. Med. Chem. 44 (2001) 3616–3621.
[9] C. Scolaro, A. Bergamo, L. Brescacin, R. Delfino, M. Cocchietto, G. Laurenczy, T.J. Geldbach, G. Sava, P.J.C. Dyson, In vitro and in vivo evaluation of ruthenium (II) – Arene PTA complexes, J. Med. Chem. 48 (2005) 4161–4171.
[10] E. Alessio, G. Balducci, A. Lutman, G. Mestroni, M. Calligaris, W.M. Attia, Synthesis and characterization of two new classes of ruthenium(III)-sulfoxide complexes with nitrogen donor ligands (L): Na[trans-$RuCl_4(R_2SO)(L)$] and mer, cis-$RuCl_3(R_2SO)(R_2SO)(L)$. The crystal structure of Na[trans-$RuCl_4(DMSO)(NH_3)$] · 2DMSO, Na [trans-RuCl, Inorg. Chim. Acta 203 (1993) 205–217.
[11] S. Thota, Anticancer ruthenium complexes in drug discovery and medicinal chemistry, Mini Rev. Med. Chem. 16 (2016) 771 e).
[12] E. Alessio, Thirty years of the drug candidate NAMI-A and the myths in the field of ruthenium anticancer compounds: a personal perspective, Eur. J. Inorg. Chem. (2017) 1549–1560.
[13] J.M. Rademaker-Lakhai, D. van den Bongard, D. Pluil, J.H. Beijnen, J.H.M. Schellens, A Phase I and pharmacological study with imidazolium-trans-DMSO-imidazole-tetrachlororuthenate, a novel ruthenium anticancer agent, Clin. Cancer Res. 10 (2004) 3717–3727.
[14] S. Leijen, S.A. Burgers, P. Baas, D. Pluim, M. Tibben, E. van Werkhoven, E. Alessio, G. Sava, J.H. Beijnen, J.H.M. Schellens, Phase I/II study with ruthenium compound NAMI-A and gemcitabine in patients with non-small cell lung cancer after first line

therapy, Investig. New Drugs 33 (2015) 201–214.
[15] E. Alessio, G. Mestroni, A. Bergamo, G. Sava, Ruthenium antimetastatic agents, Curr. Top. Med. Chem. 4 (2004) 1525–1535.
[16] G. Sava, S. Pacor, G. Mestroni, E. Alessio, Na[trans-$RuCl_4$(DMSO)Im], a metal complex of ruthenium with antimetastatic properties, Clin. Exp. Metastasis 10 (1992) 273–280.
[17] G. Sava, S. Pacor, G. Mestroni, E. Alessio, Effects of the Ru(III) complexes [mer-$RuCl_3$(DMSO)$_2$Im]degrees and Na[trans-$RuCl_4$(DMSO)Im] on solid mouse tumors, Anti Canccer Drugs 3 (1992) 25–31.
[18] G. Sava, I. Capozzi, K. Clerici, R. Gagliardi, E. Alessio, G. Mestroni, Pharmacological control of lung metastases of solid tumours by a novel ruthenium complex, Clin. Exp. Metastasis 16 (1998) 371–379.
[19] B. Gava, S. Zorzet, P. Spessotto, M. Cocchietto, G. Sava, Inhibition of B16 melanoma metastases with the ruthenium complex imidazolium trans-Imidazoledimethylsulfoxide-tetrachlororuthenate and down-regulation of tumor cell invasion, J. Pharmacol. Exp. Ther. 317 (2006) 284–291.
[20] A. Bergamo, G. Sava, Linking the future of anticancer metal-complexes to the therapy of tumor metastases, Chem. Soc. Rev. 44 (2015) 8818–8835.
[21] C.G. Hartinger, S. Zorbas-Seifried, M.A. Jakupec, B. Kynast, H. Zorbas, B.K. Keppler, From bench to bedside–preclinical and early clinical development of the anticancer agent indazolium trans-[tetrachlorobis(1H-indazole)ruthenate(III)] (KP1019 or FFC14A), J. Inorg. Biochem. 100 (2006) 891–904.
[22] A. Bergamo, A. Masi, M.A. Jakupec, B.K. Keppler, G. Sava, Inhibitory effects of the ruthenium complex KP1019 in models of mammary cancer cell migration and invasion, Met.-Based Drugs (2009) 681270.
[23] N.M. Bacac, A.C.G. Hotze, K. van der Schilden, J.G. Haasnoot, S. Pacor, E. Alessio, G. Sava, J. Reedijk, The hydrolysis of the anti-cancer ruthenium complex NAMI-A affects its DNA binding and antimetastatic activity: an NMR evaluation, J. Inorg. Biochem. 98 (2008) 402–412.
[24] M. Liu, Z.J. Lim, Y.Y. Gwee, A. Levina, P.A. Lay, Characterization of a ruthenium (III)/NAMI-A adduct with bovine serum albumin that exhibits a high anti-metastatic activity, Angew Chem. Int. Ed. Engl. 49 (2010) 1661–1664.
[25] L. Messori, A. Merlino, Ruthenium metalation of proteins: the X-ray structure of the complex formed between NAMI-A and hen egg white lysozyme, Dalton Trans. 43 (2014) 6128–6131.
[26] A. Vergara, G. D'Errico, D. Montesarchio, G. Mangiapia, L. Paduano, A. Merlino, Interaction of anticancer ruthenium compounds with proteins: high-resolution X-ray structures and Raman microscopy studies of the adduct between hen egg white lysozyme and AziRu, Inorg. Chem. 52 (2013) 4157–4159.
[27] A. Levina, A. Mitra, P.A. Lay, Recent developments in ruthenium anticancer drugs, Metall 1 (2009) 458–470.
[28] M.I. Webb, C.J. Walsby, EPR as a probe of the intracellular speciation of ruthenium (III) anticancer compounds, Metall 5 (2013) 1624–1633.
[29] J.B. Aitken, S. Antony, C.M. Weekley, B. Lai, L. Spiccia, H.H. Harris, Distinct cellular fates for KP1019 and NAMI-A determined by X-ray fluorescence imaging of single cells, Metall 4 (2012) 1051–1056.
[30] F. Barragán, D. Carrion-Salip, I. Gómez-Pinto, A. González-Cantó, P.J. Sadler, R. de Llorens, V. Moreno, C. González, A. Massaguer, V. Marchán, Somatostatin subtype-2 receptor-targeted metal-based anticancer complexes, Bioconjug. Chem. 23 (2012) 1838–1855.
[31] S.M. Meier, M. Novak, W. Kandioller, M.A. Jakupec, V.B. Arion, N. Metzler-Nolte, B.K. Keppler, C.G. Hartinger, Identification of the structural determinants for anticancer activity of a ruthenium arene peptide conjugate, Chem. Eur J. 19 (2013) 9297–9307.
[32] B.M. Blunden, D.S. Thomas, M.H. Stenzel, Macromolecular ruthenium complexes as anti-cancer agents, Polym. Chem. 3 (2012) 2964–2975.
[33] B.M. Blunden, A. Rawal, H. Lu, M.H. Stenzel, Superior chemotherapeutic benefits from the ruthenium-based anti-metastatic drug NAMI-A through conjugation to polymeric micelles, Macromolecules 47 (2014) 1646–1655.
[34] G. Mangiapia, G. D'Errico, L. Simeone, C. Irace, A. Radulescu, A. Di Pascale, A. Colonna, D. Montesarchio, L. Paduano, Ruthenium-based complex nanocarriers for cancer therapy, Biomaterials 33 (2012) 3770–3782.
[35] B. Fischer, P. Heffeter, K. Kryeziu, L. Gille, S.M. Meier, W. Berger, C.R. Kowol, B.K. Keppler, Poly(lactic acid) nanoparticles of the lead anticancer ruthenium compound KP1019 and its surfactant-mediated activation, Dalton Trans. 43 (2014) 1096–1104.
[36] P. Ringhieri, A. Pannunzio, A. Boccarelli, G. Morelli, M. Coluccia, D. Tesauro, Effect of cisplatin containing liposomes formulated by unsaturated chain-containing lipids on gynecological tumor cells, J. Lipid Res. 26 (2016) 307–312.
[37] T. Boulikas, Clinical overview on Lipoplatin: a successful liposomal formulation of cisplatin, Expert Opin. Investig. Drugs 18 (2009) 1197–1218.
[38] M.I. Webb, R.A. Chard, Y.M. Al-Jobory, M.R. Jones, E.W.Y. Wong, C.J. Walsby, Pyridine analogues of the antimetastatic Ru(III) complex NAMI-A targeting non-covalent interactions with albumin, Inorg. Chem. 51 (2012) 954–966.
[39] M.I. Webb, B. Wu, T. Jang, R.A. Chard, E.W.Y. Wong, M.Q. Wong, D.T.T. Yapp, C.J. Walsby, Increasing the bioavailability of RuIII anticancer complexes through hydrophobic albumin interactions, Chem. Eur J. 19 (2013) 17031–17042.
[40] C. Mu, S.W. Chang, K.E. Prosser, A.W.Y. Leung, S. Santacruz, T. Jang, J.R. Thompson, D.T.T. Yapp, J.J. Warren, M.B. Bally, T.V. Beischlag, C.J. Walsby, Induction of cytotoxicity in pyridine analogues of the antimetastatic Ru(III) complex NAMI-A by ferrocene functionalization, Inorg. Chem. 55 (2016) 177–190.
[41] M.E. Cucciolito, M. Trinchillo, R. Iannitti, R. Palumbo, D. Tesauro, A. Tuzi, F. Ruffo, A. D'Amora, Novel sugar-incorporated N-heterocyclic carbene containing gold (I) complexes: synthesis, characterization and cytotoxic evaluation, Eur. J. Inorg. Chem. (2017) 4955–4961.
[42] V. Benessere, M. Lega, F. Ruffo, Rational design of pseudo-enantiomeric libraries of ligands based on pyranoses for application in asymmetric catalysis, J. Organomet. Chem. 771 (2014) 105–116 (and references therein).
[43] M.S. Newman, G.T. Colbern, P.K. Working, C. Engbers, M. A, Amantea Comparative pharmacokinetics, tissue distribution, and therapeutic effectiveness of cisplatin encapsulated in long-circulating, PEGylated liposomes (SPI-077) in tumor-bearing mice, Cancer Chemother. Pharmacol. 43 (1999) 1–7.
[44] E. Alessio, G. Balducci, M. Calligaris, G. Costa, W.M. Attia, G. Mestroni, Synthesis, molecular structure, and chemical behavior of hydrogen trans-bis(dimethyl sulfoxide)tetrachlororuthenate(III) and mer-trichlorotris(dimethyl sulfoxide) ruthenium(III): the first fully characterized chloride-dimethyl sulfoxide-ruthenium(III) complexes, Inorg. Chem. 30 (1991) 609–618.
[45] M.E. Cucciolito, A. D'Amora, G. De Feo, G. Ferraro, A. Giorgio, G. Petruk, D.M. Monti, A. Merlino, F. Ruffo, Five-coordinate platinum(II) compounds containing sugar ligands: synthesis, characterization, cytotoxic activity, and interaction with biological macromolecules, Inorg. Chem. 57 (2018) 3133–3143.
[46] H. Velders, A. Bergamo, E. Alessio, E. Zangrando, J.G. Haasnoot, C. Casarsa, M. Cocchietto, S. Zorzet, G. Sava, Synthesis and chemical–pharmacological characterization of the antimetastatic NAMI-A-type Ru(III) complexes (Hdmtp)[trans-RuCl4(dmso-S)(dmtp)], (Na)[trans-RuCl4(dmso-S)(dmtp)], and [mer-RuCl3(H2O)(dmso-S)- (dmtp)] (dmtp = 5,7-Dimethyl[1,2,4]triazolo[1,5-a]pyrimidine), J. Med. Chem. 47 (2004) 1110–1121.
[47] D. Musumeci, L. Rozza, A. Merlino, L. Paduano, T. Marzo, L. Massai, L. Messori, D. Montesarchio, Interaction of anticancer Ru(III) complexes with single stranded and duplex DNA model systems, Dalton Trans. 44 (2015) 13914–13925.
[48] A. Accardo, G. Mangiapia, L. Paduano, G. Morelli, D. Tesauro, Octeotride labeled aggregates containing platinum complexes as nanovectors for drug delivery, J Pep Sci 19 (2013) 190–197.
[49] K. Matsuzaki, O. Murase, K. Sugishita, S. Yoneyama, K. Akada, M. Ueha, A. Nakamura, S. Kobayashi, Optical characterization of liposomes by right angle light scattering and turbidity measurement, Biochim. Biophys. Acta 1467 (2000) 219–226.
[50] G. Caracciolo, Clinically approved liposomal nanomedicines: lessons learned from the biomolecular corona, Nanoscale 10 (2018) 4167–4172.
[51] M. Danaei, M. Dehghankhold, S. Ataei, F. Hasanzadeh Davarani, R. Javanmard, A. Dokhani, S. Khorasani, M.R. Mozafari, Impact of particle size and polydispersity index on the clinical applications of lipidic nanocarrier systems, Pharmaceutics 10 (57) (2018) 1–17.
[52] M. Pal, U. Nandi, D. Mukherjee, Detailed account on activation mechanisms of ruthenium coordination complexes and their role as antineoplastic agents, Eur. J. Med. Chem. 150 (2018) 419–445.
[53] Z. Zhao, Z. Luo, Q. Wu, W. Zheng, Y. Feng, T. Chen, Mixed-ligand ruthenium polypyridyl complexes as apoptosis inducers in cancer cells, the cellular translocation and the important role of ROS-mediated signaling, Dalton Trans. 43 (2014) 17017–17028.